Asian Journal of Chemistry; Vol. 24, No. 8 (2012), 3707-3714

ASIAN JOURNAL OF CHEMISTRY

www.asianjournalofchemistry.co.in

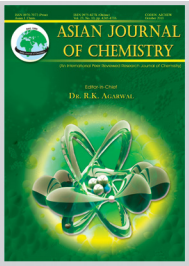

Theoretical Study on Destruction Mechanism and Kinetics of Degradation of Toluene by Ozone

ZHENGCHENG WEN[1,2,*], ZHIHUA WANG[2], JIANGRONG XU[1], JUNHU ZHOU[2] and KEFA CEN[2]

[1]College of Science, Hangzhou Dianzi University, Hangzhou 310018, P.R. China
[2]State Key Laboratory of Clean Energy Utilization (Zhejiang University), Hangzhou 310027, P.R. China

*Corresponding author: E-mail: giani@zju.edu.cn

(*Received*: 14 September 2011; *Accepted*: 23 March 2012) AJC-11222

In order to improve the technology of emission of volatile organic compounds removal by ozone, the destruction mechanism and kinetics of degradation of toluene by O_3 was investigated employing quantum chemical calculations. Theoretical results showed that, toluene was gradually degraded by O_3 *via* three times cleavages of C=C bonds. All the microcosmic reaction processes were analyzed and depicted in detail based on geometry optimizations made by the UB3LYP/6-31G(d) method. Furthermore, the kinetic parameters were also calculated by the transition state theory. The activation energy obtained by the QCISD(t)/6-311g(d,p)//UB3LYP/6-31G(d) method was 48.53 kJ/mol, which was in rough agreement with the experimental result (55.81 kJ/mol). The rate constant obtained from the transition state theory was also in good agreement with the experimental result. This indicate that the destruction mechanism and kinetics of degradation of toluene by O_3 investigated employing quantum chemical calculations in this paper was fair and reliable.

Key Words: Ozone, Volatile organic compounds, Toluene, Degradation mechanism, Kinetics, Quantum chemistry.

INTRODUCTION

Emission of volatile organic compounds (VOCs) into the atmosphere is one of the most important problems with respect to the depletion of the stratospheric ozone layer and the formation of photochemical oxidants under the presence of NOx. Moreover, even at very low concentrations[1], emission of volatile organic compounds still have great adverse effects on human health. Thus, the removal of emission of volatile organic compounds from combustion and incineration processes became an important issue for engineers and researchers. There are various emission of volatile organic compounds control methods presently available. These include thermal incineration, carbon adsorption, membrane separation, condensation, biofiltration and catalytic combustion[2-9].

As a strong oxidizer, ozone is used to remove emission of volatile organic compounds by many researchers. Regretfully, the removal efficiency of emission of volatile organic compounds by only injecting ozone was quite low. Therefore, to obtain much higher removal efficiencies, ozone was generally used in cooperation with other technologies, including catalytic incineration, carbon adsorption and ultra-violet light[10-13]. In the past few years, due to its wide application prospect, the emission of volatile organic compounds destruction by using ozone has been widely studied[10-15]. However, most of the investigations directed at the macroscopical removal efficiencies and few investigations were concerned with the microcosmic mechanisms, which radically limit the development of this technology. It is essential to the destruction mechanism and kinetics of emission of volatile organic compounds by ozone.

Because the mechanism of degrading emission of volatile organic compounds by using ozone in cooperation with other technologies is very complicated, only the mechanism of degrading emission of volatile organic compounds by using ozone alone was considered in the present work. Among various emission of volatile organic compounds, aromatic hydrocarbons are generally considered to be the priority objective for the investigations because aromatic hydrocarbons are of strong toxicity and act as precursors for the formation of polycyclic aromatic hydrocarbons (PAHs) and dioxins[16,17]. As known to all, common examples of emission of volatile organic compounds emitted from combustion and incineration processes are toluene, xylene, dichloromethane, methanol and isopropyl alcohol. Therefore, for simplicity, toluene was chosen as the representative aromatic hydrocarbon in this paper. Nowadays, quantum chemical calculation is popularly considered as a well-established method on studying chemical reactions. Therefore, the destruction mechanism and kinetic of toluene by O_3 was investigated employing quantum chemical calculations.

CALCULATIONS

Quantum chemical calculations in this study were carried out using the Gaussian suite of programs[18]. All geometries of

TABLE-1
ENERGIES OF THE STATIONARY POINTS WHEN ADDING OZONE TO TOLUENE

Stationary points	E_{UMP2} (a.u.)	$E_{QCISD(T)}$ (a.u.)	E_{ZPE} (a.u.)	$E_{tot\text{-}UMP2}$ (a.u.)	$E_{rel\text{-}UMP2}$ (kJ/mol)	$E_{tot\text{-}QCISD(T)}$ (a.u.)	$E_{rel\text{-}QCISD(T)}$ (kJ/mol)
Toluene+O_3	-495.7543	-495.7257	0.1356	-495.6187		-495.7257	
α-exo-TS	-495.7292	-495.8402	0.1375	-495.5917	70.85	-495.7027	60.40
α-exo-POZ	-495.7721		0.1404	-495.6317	-34.10		
α-endo-TS	-495.7356	-495.8448	0.1376	-495.5979	54.52	-495.7071	48.78
α-endo-POZ	-495.7706		0.1403	-495.6303	-30.61		
β-exo-TS	-495.7280	-495.8389	0.1375	-495.5906	73.95	-495.7014	63.76
β-exo-POZ	-495.7694		0.1408	-495.6286	-25.98		
β-endo-TS	-495.7333	-495.8425	0.1378	-495.5955	60.95	-495.7047	55.20
β-endo-POZ	-495.7686		0.1407	-495.6278	-24.03		
γ-exo-TS	-495.7258	-495.8375	0.1374	-495.5883	79.75	-495.7001	67.30
γ-exo-POZ	-495.7678		0.1407	-495.6272	-22.25		
γ-endo-TS	-495.7314	-495.8412	0.1377	-495.5937	65.74	-495.7035	58.26
γ-endo-POZ	-495.7671		0.1406	-495.6265	-20.40		

the reactants, products and stationary points were fully optimized by the unrestricted B3LYP method[19,20] using the 6-31G(d) basis set. The character of all stationary points was confirmed by a frequency calculation at the same level. If no imaginary frequency is shown, the stationary point was confirmed as intermediate. And if only one imaginary frequency is obtained, the stationary point was confirmed as transition state. The energies of stationary points were calculated by the UMP2/6-311g(d,p) method[21,22] based on the geometry optimizations of the UB3LYP/6-31G(d) method. After corrected with zero-point energies (E_{ZPE}), the relative energies of stationary points along the reaction processes and the activation energy (ΔE) were calculated. To improve the calculation precision, the activation energy was also calculated by the QCISD(t)/6-311g(d,p)[23,24]/UB3LYP/6-31G(d) method. Owing to average over estimation of the UB3LYP/6-31g(d) method[25], the raw calculated values of E_{ZPE} were scaled by 0.9613. For all the calculations, the spin contaminations were carefully checked and no significant spin contamination was found, which indicates that the quantum chemical calculations in this paper are reliable.

Based on the mechanism study, the reaction rate constant was calculated by the transition state theory (TST). The involved equations[26,27] are in below.

$$k(T) = \lambda\left(\frac{k_B T}{h}\right)\left(\frac{Q^{\neq}}{Q_A Q_B}\right)\exp\left(-\frac{E_a}{RT}\right)$$

$$\lambda = 1 + \frac{1}{24}\left(\frac{h\nu^{\neq}}{k_B T}\right)^2$$

here, λ is the correct factor for the quantum effect, k_B is Boltzman constant, T is the temperature, h is Planck constant, $\nu^{\neq}$ is the imaginary vibrational frequency of transition state, E_a is the activation energy, $Q^{\neq}$ and Q_A/Q_B are the total partial functions of the transition state and reactant respectively.

RESULTS AND DISCUSSION

Reaction processes: To our best of knowledge, theoretical investigations concerning the destruction mechanism of toluene by O_3 are scarce in the literature. Therefore, we use quantum chemical calculations to study the destruction reaction of toluene + O_3 in detail. The stationary points along reaction processes were optimized by the UB3LYP/6-31g(d) method and the microcosmic reaction process was analyzed. According to the cleavage of C=C bonds, the reaction process of toluene + O_3 was divided as three stages, which were discussed in the following text.

Stage I: First cleavage of C=C bond: This stage is the first and the most important stage for the overall reaction. As can be supposed from the structure of toluene, the addition of O_3 to toluene occurs in three ways *i.e.* on C=C bonds in the α-position, β-position and γ-position of the methyl group. For each adding way, we can find two mechanistically different routes: the middle O atom of O_3 is either directed away the benzene ring (exo-route) or directed toward from this ring structure (endo-route). Therefore, six similar routes can be found when adding ozone to toluene (Fig.1). Based on the geometry optimizations, energies of stationary points along the reaction process were calculated by the UMP2/6-311g(d,p) and QCISD(T)/6-311G(d,p) method respectively. Theoretical results were shown in Table-1. E_{tot} is the sum of $E_{QCISD\ (T)}$ (or E_{UMP2}) and E_{ZPE}. E_{rel} is the relative energy between the transition states and reactants. As shown in Table-1, for each additing way, the energy barrier of the endo-routes was lower than that of the exo-routes, which indicated that the endo-routes took place more easily than the exo-routes. By comparing the energy barrier in the three adding ways, the energy barrier in the α-way was lowest, which indicated that the α-way was the favoured one. Therefore, the α-endo route was believed to be the predominant route during the adding of O_3 to toluene.

For the α-endo route, the detail reaction process was calculated and depicted in Fig. 2. Firstly, the primary ozonide (α-endo-POZ) is formed *via* α-endo-TS. And then, the primary ozonide splits into intermediates (1-α-endo-M/2-α-endo-M) *via* 1-clea-endo-TS/2-clea-endo-TS. Because toluene is not a symmetrical structure, there are two ways in the cleavage of the primary ozonide: the middle O atom of the primary ozonide is directed toward either the side with methyl group or the other side. As shown in Fig. 2, the changes of geometric configurations of the stationary points can clearly describe the reaction process. During the reaction process, the distance between two attacked carbon atoms increases gradually (1.401Å→1.458Å→1.573Å→1.854Å/1.886Å→∞Å, ∞ denotes the distance exceeding the range of bond forming), which means the cleavage of C=C bond.

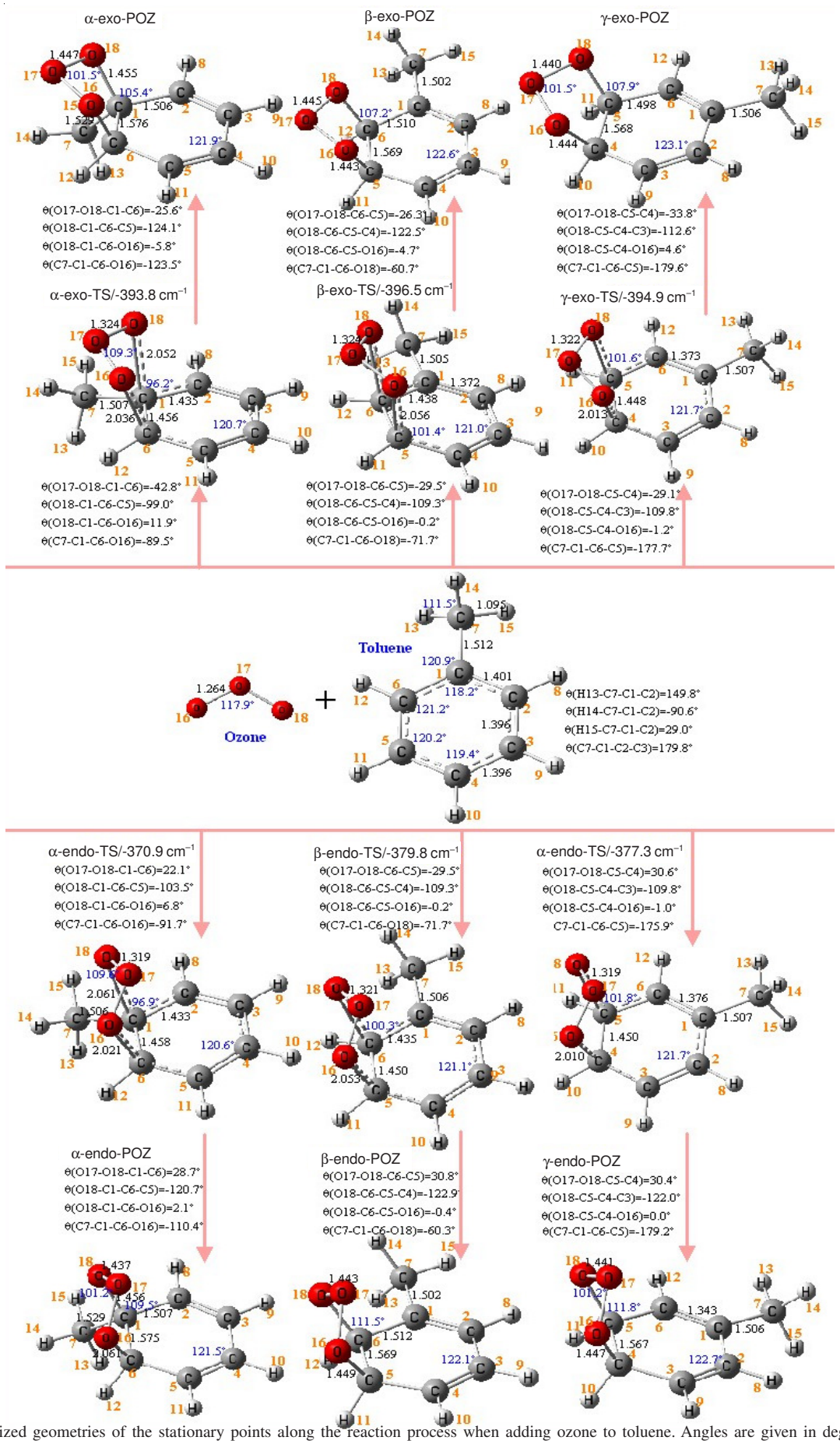

Fig. 1. Optimized geometries of the stationary points along the reaction process when adding ozone to toluene. Angles are given in degrees and bond distances are given in angstroms

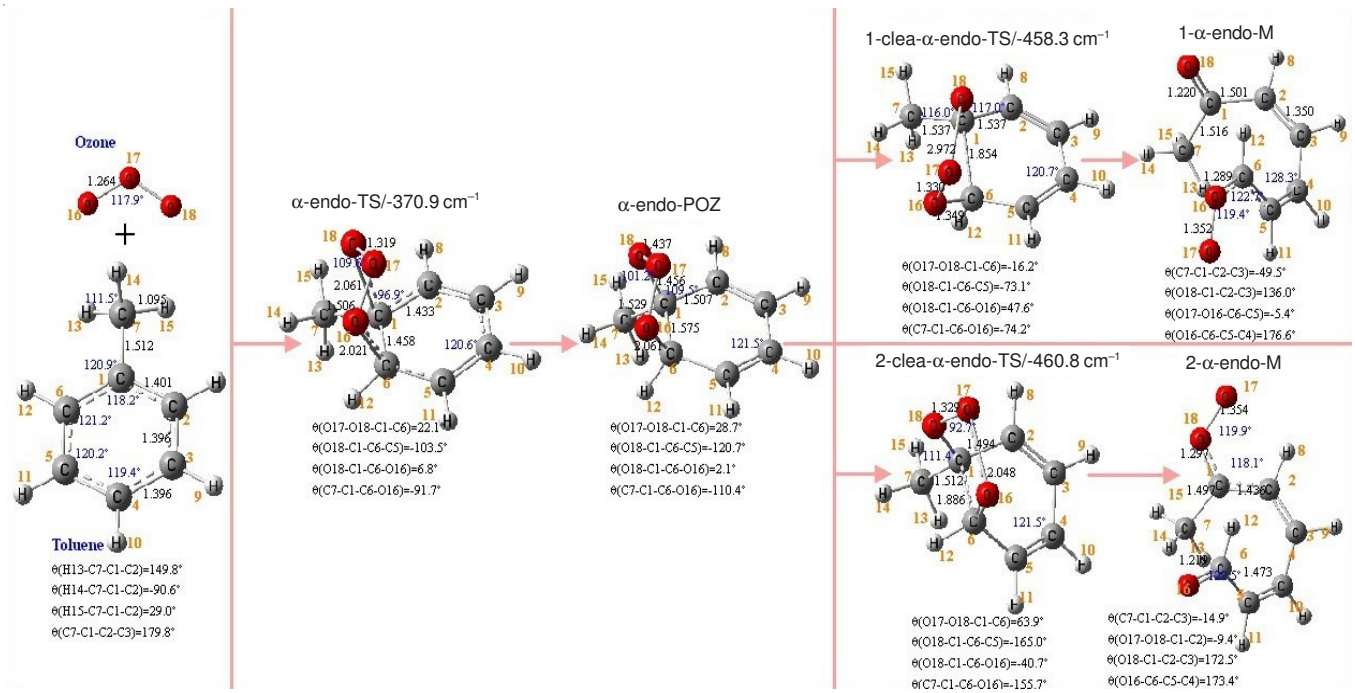

Fig. 2. Optimized geometries of stationary points along the reaction process of toluene + O_3: Stage I. Angles are given in degrees and bond distances are given in angstroms

Based on the geometry optimizations, energies of stationary points along the reaction process for the α-endo route were calculated by the UMP2/6-311g(d,p) method and the result was shown in Fig. 3. Since the energy of the primary ozonide (α-endo-POZ) was lower than that of the reactants, the primary ozonide can be believed as quite stable intermediate. From the Table-1, similar findings can be obtained in another five routes. And so, the formation of the primary ozonide can be believed as the rate-determining step for the overall reaction. Since the α-endo route was the predominant one, the formation of α-endo-POZ can be believed as the rate-determining step for the overall reaction. The calculated activation energy of the overall reaction by the UMP2/6-311g(d,p)//UB3LYP/6-31G(d) method was 54.52 kJ/mol (Fig. 3). To improve the calculation precision, the activation energy was calculated by the QCISD(t)/6-311g(d,p)//UB3LYP/6-31G(d) method and its value was 48.53 kJ/mol. As shown in Fig. 3, the energy of 2-α-endo-M was a little lower than that of 1-α-endo-M, which means that 2-α-endo-M is a little more stable than 1-α-endo-M. This indicated that 2-α-endo-M could be believed as the favoured product from the first cleavage of C=C bond.

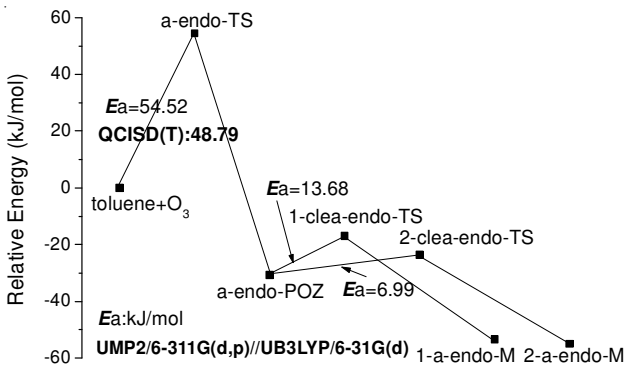

Fig. 3. Relative energies of stationary points along the reaction process of toluene + O_3: Stage I

Stage II: Second cleavage of C=C bond: Since 2-α-endo-M was believed as the favoured product from the first cleavage of C=C bond, 2-α-endo-M was chosen as the reactant for the second cleavage of C=C bond. As shown in Fig. 4, two C=C bonds can be found in the structure of 2-α-endo-M. Therefore, the adding of O_3 to 2-α-endo-M occurs in two ways *i.e.* on 2,3-C=C and 4,5-C=C bonds. Similar to the stage I, there are two mechanistically different routes in the adding of O_3 to 2-α-endo-M: the middle O atom of O_3 is either directed away (exo-route) or directed toward from (endo-route) the ring structure. And so, four similar routes can be found in the adding of ozone to 2-α-endo-M (Fig. 4). For each route, the primary ozonide of 2-α-endo-M is formed *via* a transition state firstly; and then, the primary ozonide splits into various carbonyl oxides *via* another transition states. There are two ways in the cleavage of the primary ozonide: the middle O atom of the primary ozonide is directed toward either the side with four C atoms or the side with two C atoms. Similar to the route in the stage I, the changes of geometric configurations can describe the reaction process of each route clearly.

For the stage II, the energies of stationary points were calculated by the UMP2/6-311G(d,p)//UB3LYP/6-31G(d) method and the energies variation along the reaction process was shown in Fig. 5. For the four similar routes, the energies of the primary ozonides were much lower than that of the reactants, which indicated that the primary ozonides were the stable intermediates. Therefore, similar to the stage I, the formation of the primary ozonide was the rate-determining step for this stage. However, the calculated energies of the transition states were lower than that of the reactants. This anomalous behaviour could be ascribed to energy values referred to non-equilibrium geometries because the energies of these transition states were calculated by UMP2/6-311G(d,p) based on the geometries optimized of UB3LYP/6-31G(d). If the reaction is nearly barrierless, this anomalous behaviour often occurs.

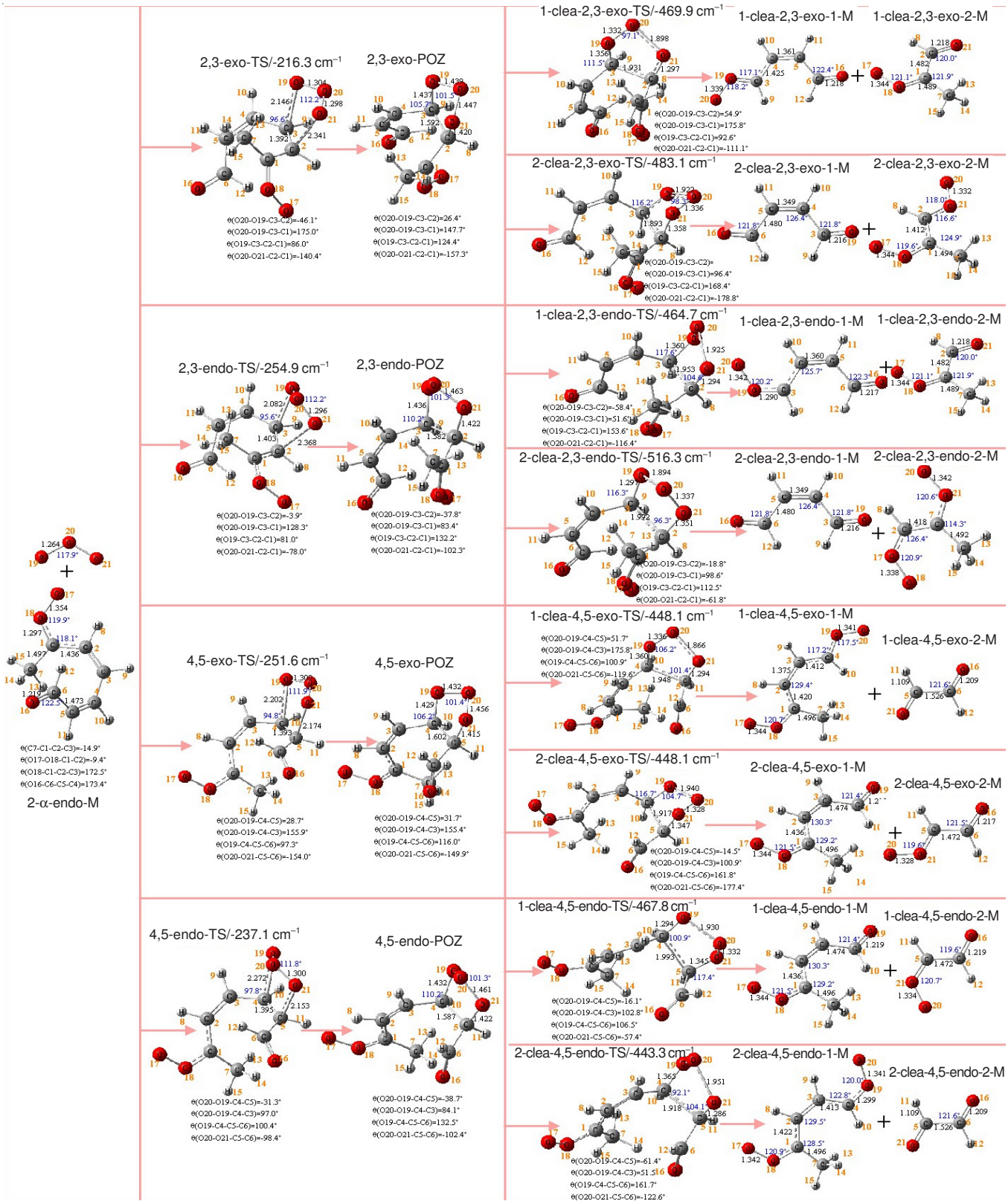

Fig. 4. Optimized geometries of stationary points along the reaction process of toluene + O_3: Stage II. Angles are given in degrees and bond distances are given in angstroms

Based on the above analysis, the formation of the primary ozonide in stage II could be considered as a direct reaction and its activation energy can be believed as 0 kJ/mol. And so, by comparing, the activation energy of the stage II (0 kJ/mol) was much smaller than that of the stage I (54.52 kJ/mol). That is to say, the second C=C bond was much easier to destruct than the first C=C bond. The reason for this fact may be that, toluene is more stable because of its aromatic ring structure and the 2-α-endo-M is much easier to destruct because of its chain structure.

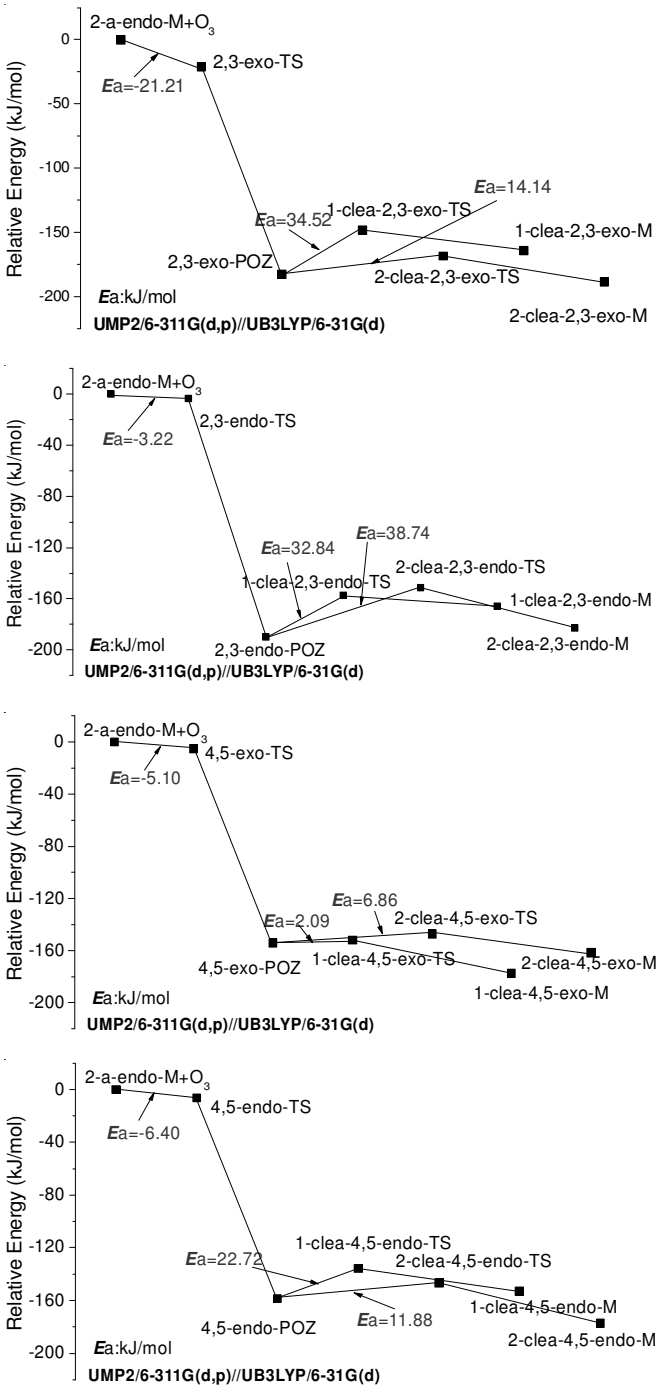

Fig. 5. Relative energies of stationary points along the reaction process of toluene + O_3: Stage II

Stage III: Third cleavage of C=C bond: After the second cleavage of C=C bond in the stage II, toluene splits into various carbonyl oxides. Those carbonyl oxides with four C atoms also have a C=C bond (Fig. 6). For the simplicity, only a carbonyl oxide (1-clea-4,5-endo-1-M) was chosen as an example for the third cleavage calculation (Fig. 6). Similar to the adding of O_3 in the stage I and II, the addition of O_3 to 1-clea-4,5-endo-1-M has two mechanistically different routes: the middle O atom of O_3 is either directed away (exo-route) or directed toward from (endo-route) the ring structure with four C atoms. Furthermore, the reaction process for each route is quite similar to that of the route in the stage I and II and the reaction process of each route can be clearly described by the changes of geometric configurations of the stationary points. Similar to the stage I and II, the energies variation along the reaction process in the stage III were obtained by the UMP2/6-311g(d,p)//UB3LYP/6-31G (d) method and shown in Fig. 7. Similar to the stage II, the formation of the primary ozonide was believed as the rate-determining step for this stage and its activation energy was 0 kJ/mol. This indicated that, the 1-clea-4,5-endo-1-M in the stage III is very easy to destruct because of its chain structure, which is similar to the 2-α-endo-M in the stage II.

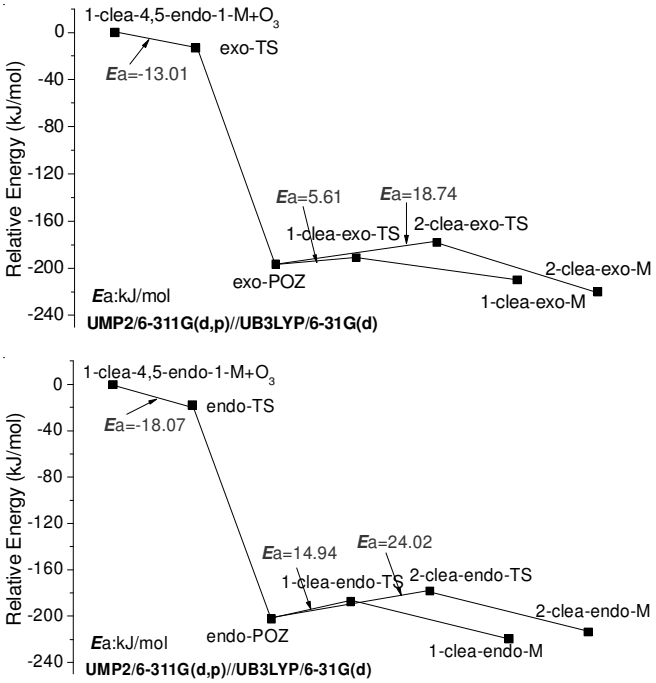

Fig. 6. Relative energies of stationary points along the reaction process of toluene + O_3: Stage III

As shown in Figs. 2 and 3, after the three times cleavage of C=C bonds, toluene splits into various carbonyl oxides such as glyoxal. And also, OH was produced via the isomerization of those carbonyl oxides with three or four O atoms[28]. Therefore, a series of complicated reactions were initiated by the carbonyl oxides, O_3 and OH. And at last, smaller radicals and molecules, such as CO_2, O_2, OH and aldehydes, were produced. In the Toby's experiment[28], CO_2, OH and glyoxal was also found as products. This indicated the mechanism study by using quantum chemical calculations is fair and reliable.

Kinetic study: As has been said, the formation of α-endo-POZ of toluene was believed as the rate-determining step for the overall reaction and the calculated activation energy by the UMP2/6-311g(d,p)//UB3LYP/6-31G(d) method was 54.52 kJ/mol. To improve the calculation precision, the activation energy was also calculated by QCISD(t)/6-311g(d,p)//UB3LYP/6-31G(d) and its value was 48.53 kJ/mol. This result was lower than the experimental result (55.81 kJ/mol)[28]. For calculating the pre-exponential factor (A), the total partial function of transition state (α-endo-TS) and the reactants (toluene + O_3) were calculated at the UB3LYP/6-31G(d) level: $Q^{\neq}$ (α-endo-TS): 2.29×10^{17} L mol^{-1} s^{-1}, Q_A (toluene): 2.87×10^{15} L mol^{-1} s^{-1}, Q_B(O3): 4.37×10^{10} L mol^{-1} s^{-1}. The pre-exponential factor obtained from theoretical calculation was 4.18

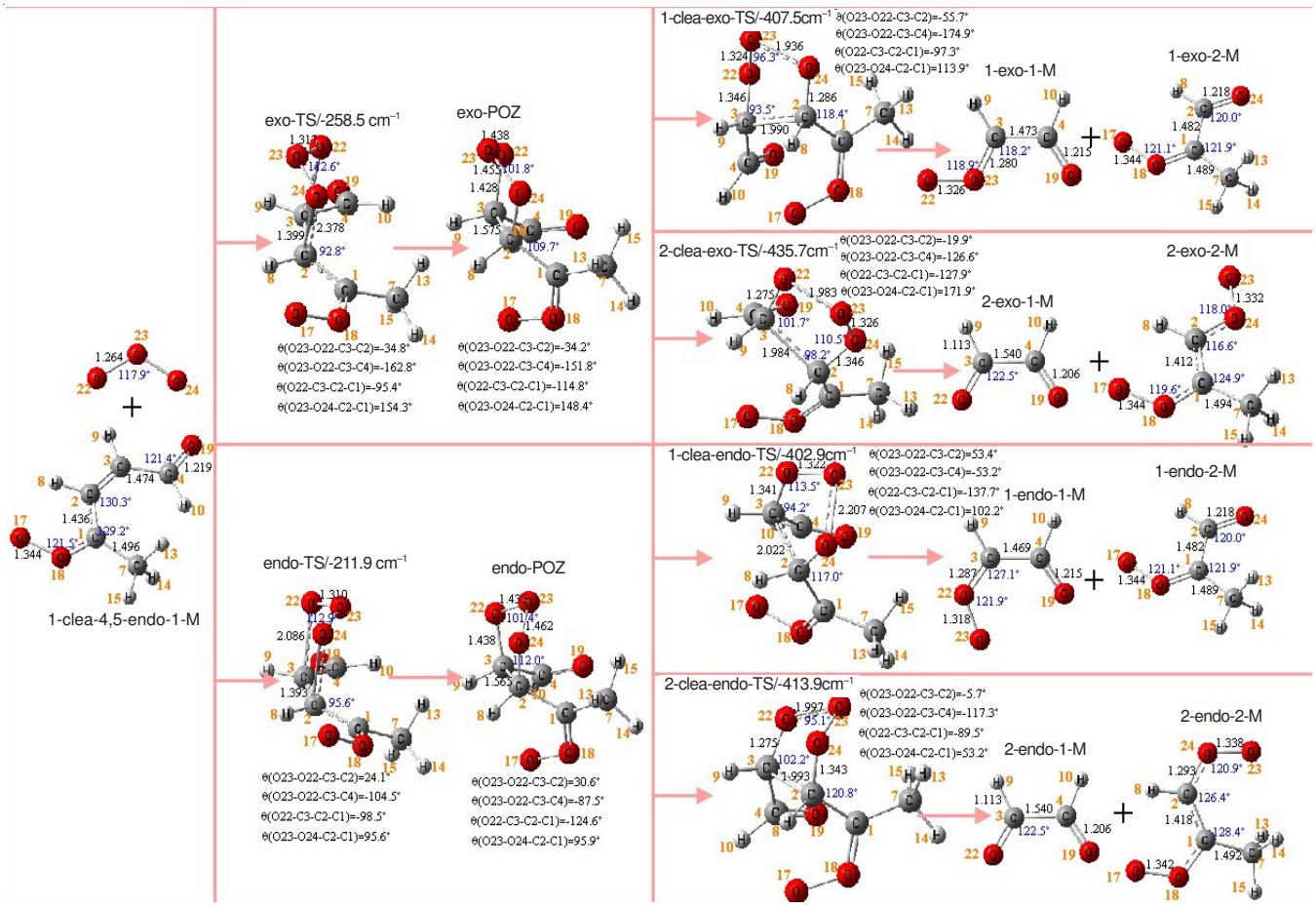

Fig. 7. Optimized geometries of stationary points along the reaction process of toluene + O_3: Stage III. Angles are given in degrees and bond distances are given in angstroms

$\times 10^{10}$ $cm^3mol^{-1}s^{-1}$, which was lower than the experimental result (1.41×10^{12} cm^3 $mol^{-1}s^{-1}$)[28]. Moreover, the rate constant of the toluene + O^3 reaction was calculated and shown in Fig. 8. By comparison with the theoretical result, the rate constant derived from the experiment[28] was more sensitivity with the temperature. This may be ascribed to the lower experimental activation energy in comparison with the theoretical value. However, this theoretical result was still in agreement with the experimental result[28].

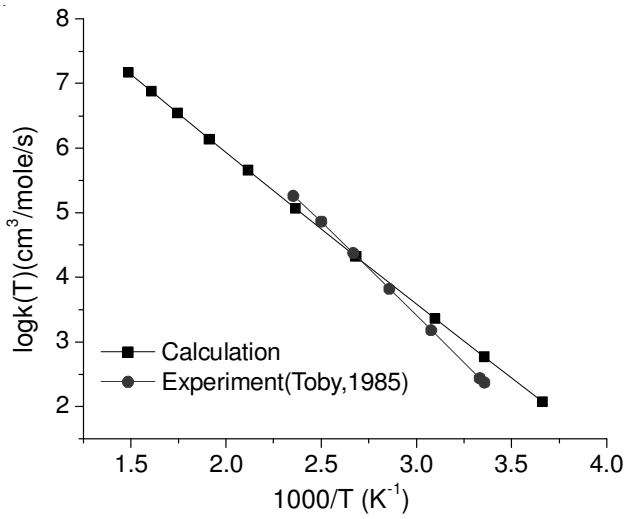

Fig. 8 the rate constant k calculated from TST

Conclusion

The destruction mechanism and kinetic of toluene by O_3 was investigated employing quantum chemical calculations in detail in this paper. The products, activation energy and rate constant obtained from quantum chemical calculation was in agreement with the experimental result. This indicated that the mechanism and kinetic investigation by using quantum chemical calculations was fair and reliable. The theoretical results in this paper can be believed to lay an important foundation for the further research on aromatic hydrocarbons and other emission of volatile organic compounds removal by using O_3.

ACKNOWLEDGEMENTS

The authors acknowledged the financial support of the Key Project of the National Natural Science Foundation of China (Grant No. 51006030).

REFERENCES

1. V.J. Feron and J.P. Groten, *Food Chem. Toxicol.*, **40**, 825 (2002).
2. J.H. Kim, J.H. An, Y.S. La, J.S. Jung, H.M. Jeong, S.M. Kim, N.G. Moon, B.W. Lee, Y.H. Yoon and Y.I. Choi, *J. Ind. Eng. Chem.*, **14**, 194 (2008).
3. J.V. Durme, J. Dewulf, C. Leys and H. Langenhove, *Appl. Catal. B: Environ.*, **78**, 324 (2008).
4. Ch. Subrahmanyam, A. Renken and L. Kiwi-Minsker, *Chem. Eng. J.*, **134**, 78 (2007).
5. M. Guillemot, J. Mijoin, S.M. Mignard, J. Guillemot, S. Mijoin and P. Mignard, *Appl. Catal. B: Environ.*, **75**, 249 (2007).

6. B. Ozturk and D. Yilmaz, *Process Safety and Environ. Protect.*, **84(B5)**, 391 (2006).
7. D. Debasish, G. Vivekanand and V. Nishith, *Carbon*, **42**, 2949 (2004).
8. B. Guieysse, C. Hort, V. Platel, R. Munoz, M. Ondarts and S. Revah, *Biotechnol. Adv.*, **26**, 398 (2008).
9. K. Everaert and J. Baeyens, *J. Hazard. Mater. B*, **109**, 113 (2004).
10. C.W. Kwong, Y.H. Christopher, K.S. Hui and M.P. Wang, *Atmosph. Environ.*, **42**, 2300 (2008).
11. S. Kazuhiko, S. Aya and S. Kazuhiko, *Catal. Commun.*, **4**, 247 (2003).
12. A. Gervasini, G.C. Vezzoli and V. Ragaini, *Catal. Today*, **29**, 449 (1996).
13. Y.S. Shen and K. Young, *Chemosphere*, **38**, 1855 (1999).
14. Z. Fan, P. Lioy, C. Weschler, N. Fiedler, H. Kipen and J. Zhang, *Environ. Sci. Technol.*, **37**, 1811 (2003).
15. C.J. Weschler, *Indoor Air*, **10**, 269 (2000).
16. V.K. Everaert and J. Baeyens, *Chemosphere*, **46**, 439 (2002).
17. M.Y. Wey, J.C. Chen, H.Y. Wu, W.J. Yu and T.H. Tsai, *Fuel*, **85**, 755 (2006).
18. M.J. Frisch, G.W. Trucks and J.A. Pople, Gaussian 03. Gaussian, Inc., Pittsburgh, PA (2003).
19. C. Lee, W. Yang and R.G. Parr, *Phys. Rev. B*, **37**, 785 (1988).
20. A.D. Becke, *J. Chem. Phys.*, **98**, 5648 (1993).
21. C. Gonzalez and H.B. Schlegel, *J. Chem. Phys.*, **90**, 2154 (1989).
22. M.J. Frisch, M. Head-Gordon and J.A. Pople, *Chem. Phys. Lett.*, **166**, 275 (1990).
23. J. Gauss and C. Cremer, *Chem. Phys. Lett.*, **150**, 280 (1988).
24. E.A. Salter, G.W. Trucks and R.J. Bartlett, *J. Chem. Phys.*, **90**, 1752 (1989).
25. A.P. Scott and L. Random, *J. Phys. Chem.*, **100**, 16502 (1996).
26. M. Dupuis, G. Fitzgerald, B. Hammond and W.A. Lester, *J. Chem. Phys.*, **84**, 2691 (1986).
27. D. Hwang and A.M. Mebel, *J. Chem. Phys.*, **109**, 10847 (1998).
28. S. Toby, L.J. Van de Burgt and F.S. Toby, *J. Phys. Chem.*, **89**, 1982 (1985).